

DRIVEABILITY ANALYSIS  
OF MODEL PILES  
IN CLAY

---

Presented to  
The Faculty of the Department of Civil Engineering  
The University of Houston

---

In Partial Fulfillment  
of the Requirements for the Degree  
Master of Science in Engineering (Undifferentiated)

---

by  
Edward H. Peterson  
December, 1977

## ACKNOWLEDGMENTS

The compilation of this thesis would not have been possible without the dedication and assistance of many people. The greatest debt of gratitude is due to Dr. Michael W. O'Neill for his assistance and constant encouragement, and to Mr. Norm Peterson for his assistance in the design and implementation of the data acquisition system. Special thanks is also due to my fellow graduate students, Azaroghly Yazdanbod, and to the members of the student chapter of the A.S.C.E. for their timely assistance.

Finally, I wish to express my deepest appreciation to my wife, Debbi, for her constant support and encouragement, without whom this work could not have been completed.

DRIVEABILITY ANALYSIS  
OF MODEL PILES  
IN CLAY

---

An Abstract of a Thesis  
Presented to  
The Faculty of the Department of Civil Engineering  
The University of Houston

---

In Partial Fulfillment  
of the Requirements for the Degree  
Master of Science in Engineering (Undifferentiated)

---

by  
Edward H. Peterson  
December, 1977

## ABSTRACT

### DRIVEABILITY ANALYSIS OF MODEL PILES IN CLAY

This thesis contains the results of a driveability analysis on two model piles driven into compacted clay soils. Two different soils are used to represent reasonable upper and lower limits to liquid limit and plasticity index of Recent deposits found in the Gulf of Mexico. The model piles were instrumented to measure the compressive stress wave as it traveled down the pile after the hammer impact. A wave equation analysis was performed to determine values of the side damping parameter ( $J_m$ ) that resulted in the best correlation with measured stress ratios and blow counts. A theory is presented that proposes that the magnitude of the damping parameter is a function of the frequency of the soil loading by the stress wave in the pile.

## TABLE OF CONTENTS

Chapter		Page
I.	INTRODUCTION . . . . .	1
	GENERAL. . . . .	1
	THE COMPUTER PROGRAM . . . . .	3
II.	TEST SOILS . . . . .	8
III.	TESTING PROGRAM. . . . .	22
	INSTRUMENTATION. . . . .	22
	TESTING FRAME AND SOIL COLUMN. . . . .	23
	DRIVING SYSTEM . . . . .	26
	LOADING SYSTEM . . . . .	30
	TESTING PROCEDURES . . . . .	31
IV.	PRESENTATION OF RESULTS. . . . .	35
V.	DISCUSSION AND RECOMMENDATIONS . . . . .	45
	BIBLIOGRAPHY . . . . .	52
	APPENDIX I . . . . .	54

# CHAPTER I

## INTRODUCTION

### General

The purpose of the study reported herein was to determine experimentally the viscous damping that occurs during driving of long, slender pipe piles penetrating uniform clay. The effect of damping and of distribution of soil resistance on the driveability predictions for such piles were determined with the wave equation technique, using a computer program developed at Texas A and M University (Ref. 6).

Model pile tests were conducted on two instrumented steel pipe piles, 100 inches long, 1 inch in diameter, with a 0.096-inch wall. The piles were driven into two compacted clay soils. Soil I was a pure kaolinite with a plasticity index ( $I_p$ ) of 23. The second soil was a mixture of 10% montmorillonite and 90% kaolinite with an  $I_p$  of 37. A detailed description of the other soil properties is given in Chapter 2.

It was the intent of this testing program to model as closely as possible the long, slender piles used in off shore structures. It was recognized that it would not be possible in these small scale tests to model either the total or the effective stress states that exist along

an actual off shore pile, which may be up to 1,000 feet long. However, the relative stiffness of the pile and soil in the model tests could be maintained in the range of that found for piles driven into the deep deposits of normally consolidated to under-consolidated clay soils found in the Gulf of Mexico. For this testing program, the relative stiffness was defined as the ratio of the pile flexibility to the vertical elastic displacement of the soil produced by skin friction.

$$\text{The pile flexibility} = \frac{QL}{AE_p} = \frac{4 QL}{E_p \pi (d^2 - d_i^2)}$$

Where: Q = Applied load

L = Depth of embedment of pile

A = Cross-sectional area

$E_p$  = Modulus of elasticity of the pile

d = Outside diameter of the pile

$d_i$  = Inside diameter of the pile

$$\text{Elastic displacement of the soil} = \frac{fd}{E_s} = \frac{Qd}{\pi dL E_s}$$

Where: f = Unit side shear stress (uniform)

$E_s$  = Modulus of elasticity of the soil

$$\text{Relative stiffness} = \frac{E_s (L^2)}{E_p (d^2)} \frac{1}{1 - (d_i/d)^2}$$

A typical pile used in the Gulf of Mexico might be described by the following parameters:

$$d = 48''$$

$$d_i = 45'' \text{ (} 1\frac{1}{2}'' \text{ average wall thickness)}$$

$$L = 200 \text{ ft.}$$

$$E_p = 29 \times 10^6 \text{ psi}$$

$$E_s = 700 \text{ psi}$$

These parameters yield a relative stiffness or approximately 0.5. The range of relative stiffness obtained in the models in this study was from 0.1 at a shallow penetration of 25 inches to 0.4 at maximum penetration. Thus, the models represent the typical pile-soil stiffness reasonably well for a Gulf of Mexico application.

During the testing program, the load-settlement relationships, load-distribution relationships, compression wave propagation in the pile, blow counts, and hammer energy were all measured. These data, along with the physical characteristics of the pile, formed the input data for the wave equation program. No attempt was made to alter the analytical model used in the computer program.

#### The Computer Program

The computer program is based on idealizing the actual pile-hammer-soil system as a series of concentrated weights, springs, and viscous dampers. The ram and helmet are assumed to be concentrated masses between which a spring representing

the stiffness of the cushion is inserted. The pile is idealized as a series of concentrated weights connected by weightless springs.

The pile is assumed to move through the soil without moving the adjacent soil mass. The soil resistance is represented by springs and dash pots. The solution to the idealized pile driving problem is accomplished using the technique developed by Smith (Ref. 11). The algorithm is a finite difference technique that approximates the velocities, displacements, and forces on each element of the pile during successive time increments.

The complete algorithm is represented by the following equations:

$$D(m, t) = D(m, t-1) + 1/2 \Delta t V(m, t-1) \quad (1)$$

$$C(m, z) = D(m, t) - D(m+1, t) \quad (2)$$

$$F(m, t) = C(m, t) K(m) \quad (3)$$

$$R(m, t) = \{D(m, t) - D'(m, t)\} K'(m) \{1 + J(m) V(m, t-1)\} \quad (4)$$

$$V(m, t) = V(m, t-1) + \{F(m-1, t) - F(m, t) - R(m, t)\} g \Delta t / W(m) \quad (5)$$

where  $m$  = the mass number;

$t$  = the time interval number;

$\Delta t$  = the time interval (sec.);

$D(m, t)$  = total displacement of mass number  $m$  during time interval  $t(m)$ ;

$V(m,t)$  = velocity of mass  $m$  during time interval  $t$  (ft/sec) (assumed constant);

$C(m,t)$  = compression of spring  $m$  during time interval  $t$  (in);

$F(m,t)$  = force in spring  $m$  during time interval  $t$  (lb);

$K(m)$  = spring constant of mass  $m$  (lb/in);

$R(m,t)$  = soil resistance acting on mass  $m$  during time interval  $t$  (lb/in);

$K'(m)$  = spring constant for the soil acting along mass  $m$  (lb/in);

$D'(m,t)$  = inelastic soil displacement along mass  $m$  during time interval  $t$  (in);

$J(m)$  = damping constant acting along mass  $m$  (sec/ft);

$W(m)$  = weight of mass  $m$  (lb);

$g$  = acceleration due to gravity (ft/sec<sup>2</sup>).

In the solution, the pile is assumed to be initially unstressed and at rest. The values and distribution of the maximum soil resistances and damping are known or assumed, and the weight and velocity of the ram just prior to impact are known. The inelastic nature of the cushion material and the energy losses on impact of the ram with the pile are accounted for by the coefficient of restitution. In these tests, no cushion materials were used, in order to eliminate one source of uncertainty in the computer simula-

tion. The energy losses on impact of the ram with the driving plate were accounted for by using a coefficient of restitution of 0.95. This value seemed reasonable since the driving was done at such low energies and little plastic deformation occurred.

The computer solution is started by applying the ram velocity to mass number one (the ram) at time  $t=1$ . All values of the other variables are calculated at that time increment using equations 1 - 5. The time increment is increased, and the values of the variables are recalculated. The computer solution proceeds until the inelastic displacements of all the pile segments are less than some predetermined value. The total set of the pile under that one blow of the hammer is then the inelastic displacement at the tip of the pile.

In this algorithm, the soil properties are accounted for in the equation for  $R(m,t)$ , the soil resistance acting on mass segment  $m$  during time interval  $t$ . The quantity  $K'(m)$ , the soil spring constant, is the ratio of the ultimate soil resistance ( $R_u$ ) to the maximum elastic displacement (or "quake") of the soil ( $Q$ ). The term  $J(m)$  represents the viscous damping coefficient for the soil at mass  $m$ .

These three parameters represent the entire input to the algorithm necessary to describe the response of the

soil to the penetrating pile. The value of  $R_u$  most often used is the static load capacity of the pile measured during a load test. This value, for piles driven in clay, can be several times the actual capacity during driving due to the disturbance of the soil caused during driving. Since the actual soil resistance during driving cannot be measured, this approximation was used in the current analysis. The soil quake can be estimated from the load-settlement curves. For this analysis, the quake along the side of the pile was taken to be the value of top displacement at which the load settlement curve started to become nonlinear. The value of quake at the tip of the pile was taken as the top displacement at which plunging of the pile occurred. The values chosen for the computer analysis were average values for all the static load tests run. The damping factor  $J(m)$  was the only soil parameter which could not be estimated from either the driving data or static load test data. During the computer analysis, therefore, values of  $J$  were determined by varying the average value and distribution of  $J$  along the pile, until the computed values of stresses and blow counts both became approximately equal to those measured in the testing program.

## CHAPTER II

### TEST SOILS

Two test soils were used, representing reasonable upper and lower limits to liquid limit and plasticity index found in Recent deposits in the Gulf of Mexico. Each soil was placed in a test chamber 22 inches in diameter and 105 inches high by compaction. The soils were compacted at near standard Proctor effort at a water content several percent wet of optimum in order to effect as high a degree of saturation as possible. The soils were uniformly compacted in thin layers by a procedure described later to achieve a uniform undrained shear strength throughout the test chamber. The first test was conducted in a kaolin soil, commercially available under the name Kaolin-P. The indices and standard Proctor compaction curve are shown in Fig. 1. Also indicated on that figure is the compaction water content of 39% and the degree of saturation contours. The compaction water content corresponds to a degree of saturation of approximately 90%. The clay is classified as MH according to the Unified Soil Classification System. As may be seen in Fig. 2, the limit values plot just below the A-line on the Plasticity Chart, which is a typical phenomenon for kaolin clays.

The second test was conducted in a soil made of a mixture of 90% kaolin and 10% montmorillonite. The montmoril-

FIGURE 1  
Compaction Curve  
Soil 1

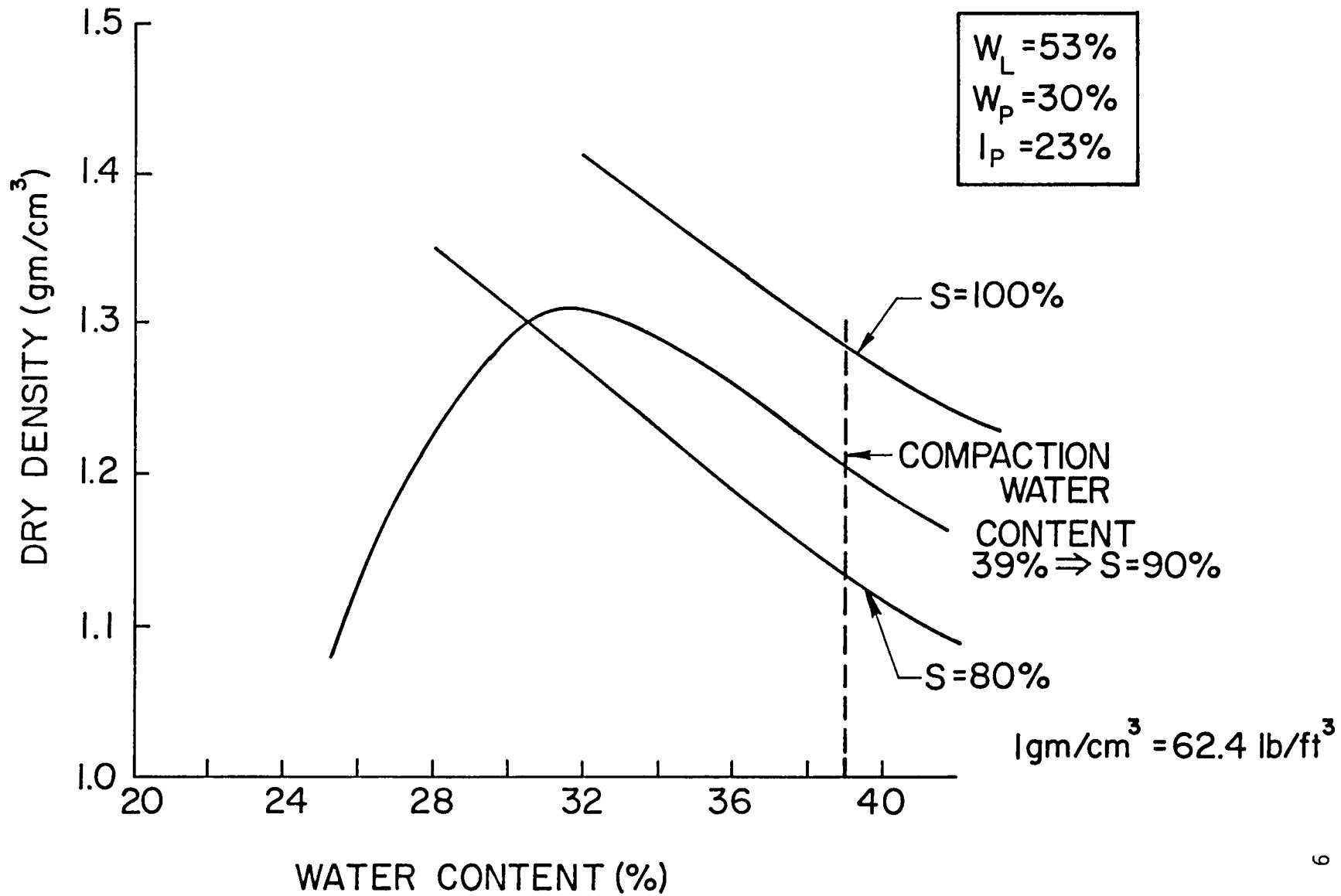
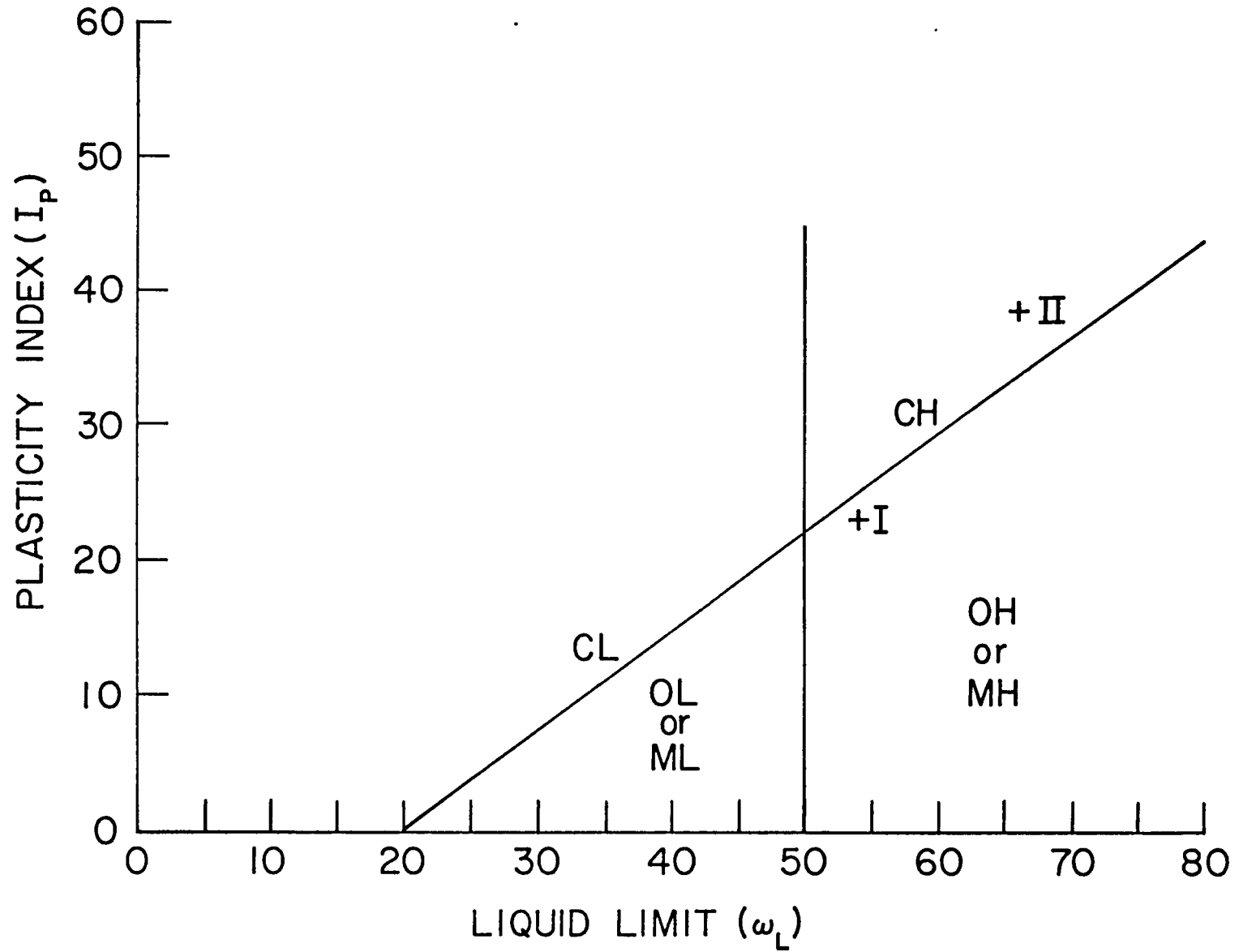


FIGURE .2

Plasticity Chart



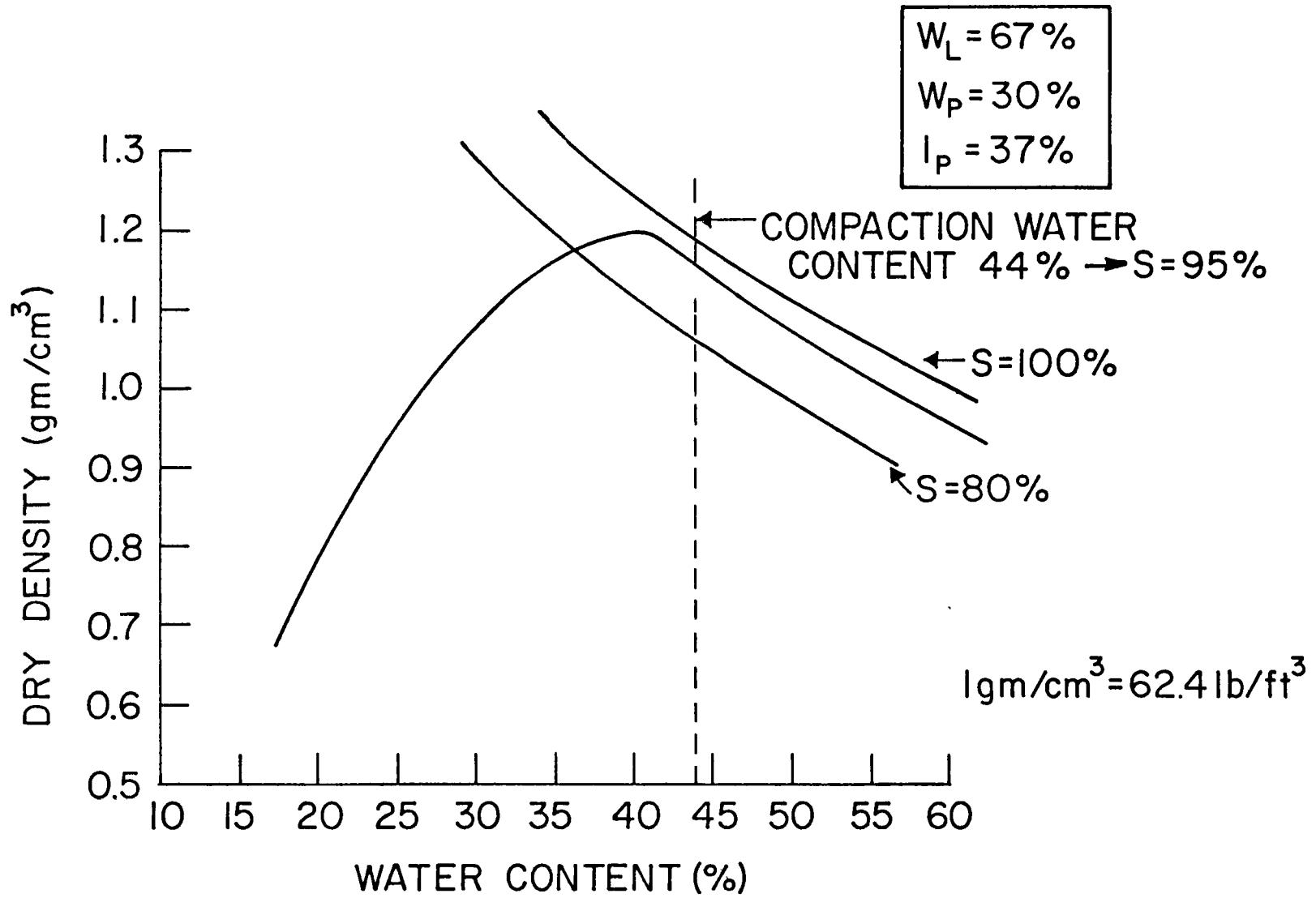
lonite was purchased commercially under the name of Bascogel. The limits and the standard Proctor compaction curve for this soil are shown in Fig. 3. Also shown is the compaction water content of 43%, indicating again that approximately 90% saturation was achieved. This soil had a higher plasticity index and liquid limit than the kaolin soil used in the first test. Its limits plotted above the A-line, as shown in Fig. 2, and it is classified as a CH clay in the Unified Soil Classification System. For a detailed chemical analysis of the Kaolin-P and Bascogel, see Appendix 1.

Variations of shear strength were obtained after the respective tests were concluded. Each column of soil was carefully sampled several inches away from the position of the pile as the soil was removed. Sampling was accomplished at several levels with a 1.25-inch diameter by 6-inch long thin-walled tube. Miniature vane tests, unconsolidated undrained (UU) triaxial compression tests for undisturbed soil, and consolidated undrained (CU) triaxial compression tests for remolded soil were conducted on the samples. Water content was measured at several levels to verify that the soil was at the intended degree of saturation.

The confining pressure for the CU triaxial tests was established at three psi, which was estimated to be the approximate average normal pressure in the center of the test vessel before the piles were driven, and it was assumed that the

FIGURE 3

Compaction Curve  
Soil 1



remolded soil would have consolidated under no more than three psi confining pressure in a period of 24 hours (the waiting time between driving and final pile testing) because the soil was not completely saturated. The confining pressures for the UU triaxial tests were maintained at 10 psi. This value of confining pressure was selected as a convenience for testing purposes. Measured variations in shear strength and water content for the two test soils are given in figs. 4 through 7. Idealized values are shown as dashed curves.

Note that the soil was maintained at a medium-stiff to stiff consistency in order to keep the relative stiffness within the range of typical Gulf of Mexico offshore piling. The value of the elastic modulus for the soil, which was needed for verification of relative stiffness, was taken from the initial portion of the CU triaxial test curves for the remolded soil, figs. 8 and 9. Corresponding curves for the UU tests are shown in figs. 10 and 11.

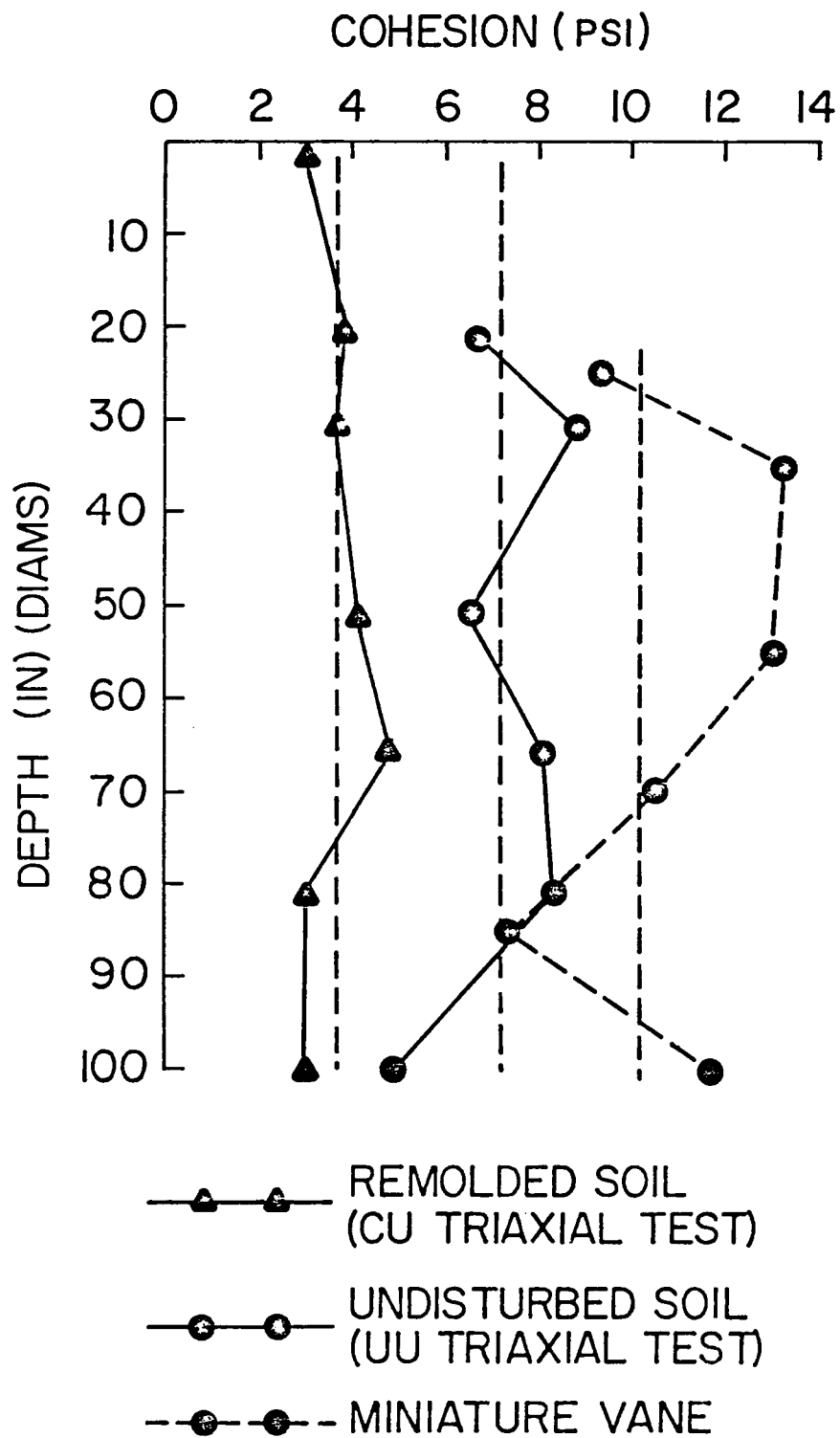


FIGURE 4

Strength Profile  
Soil 1

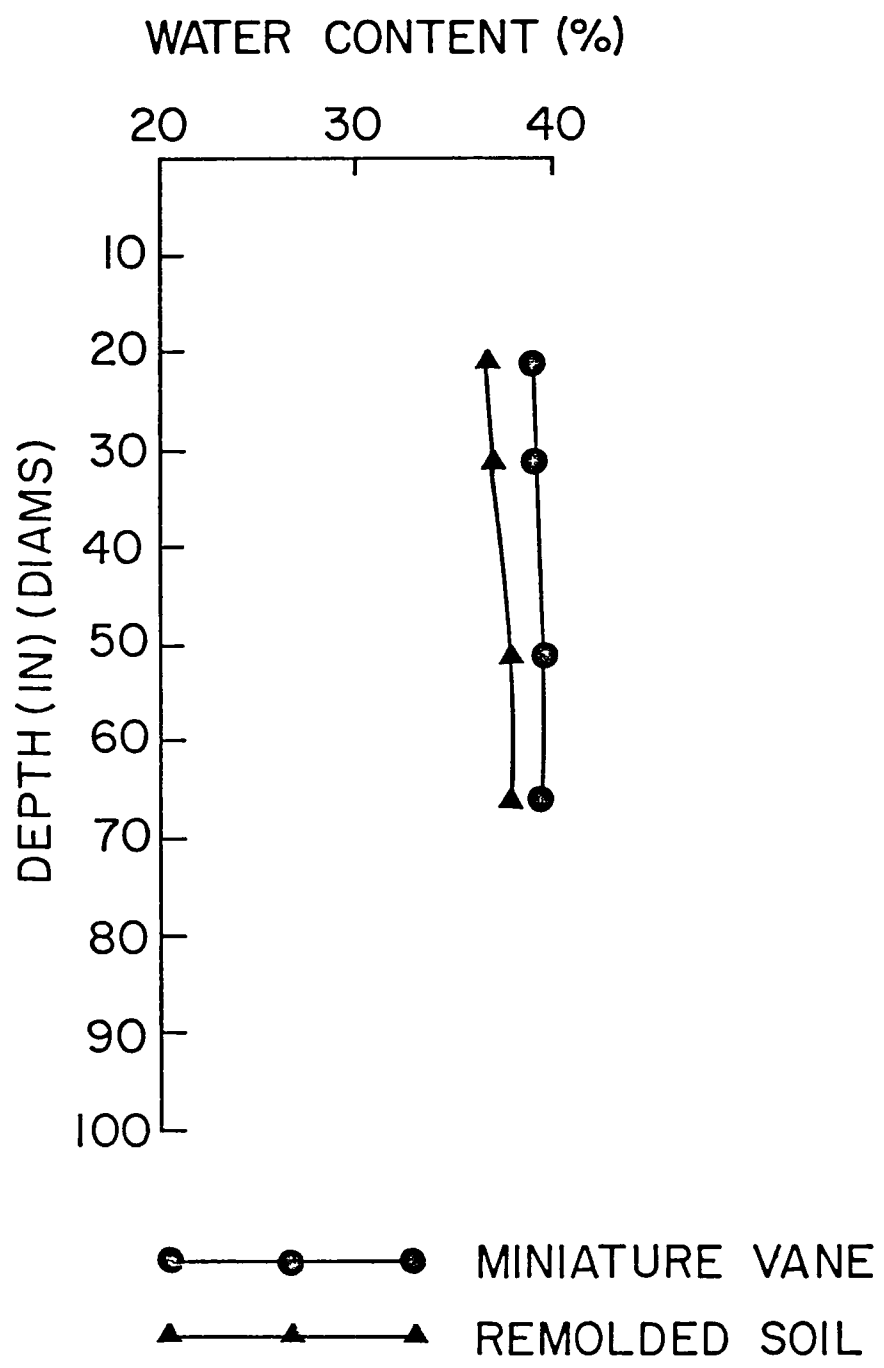
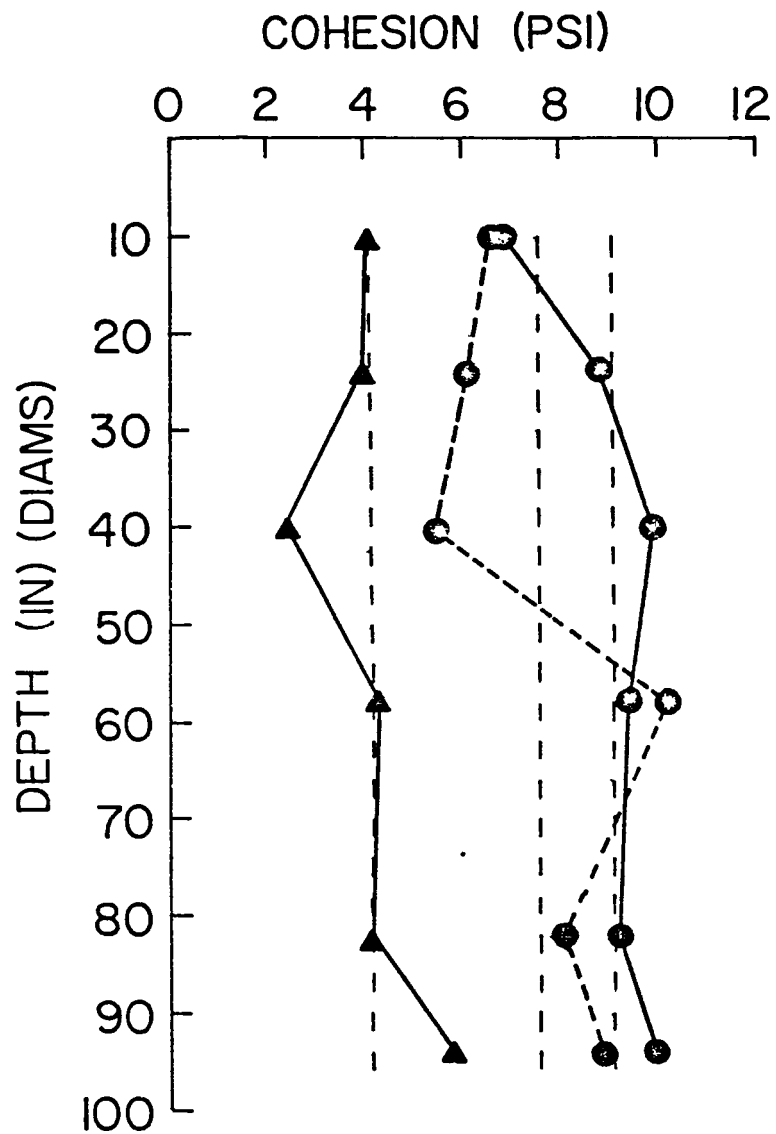


FIGURE 5

Water Content Profile  
Soil 1



- ▲—▲ REMOLDED SOIL (CU TRIAXIAL TEST)
- UNDISTRIBUTED SOIL (UU TRIAXIAL TEST)
- -○ MINIATURE VANE

FIGURE 6

Strength Profile  
Soil II

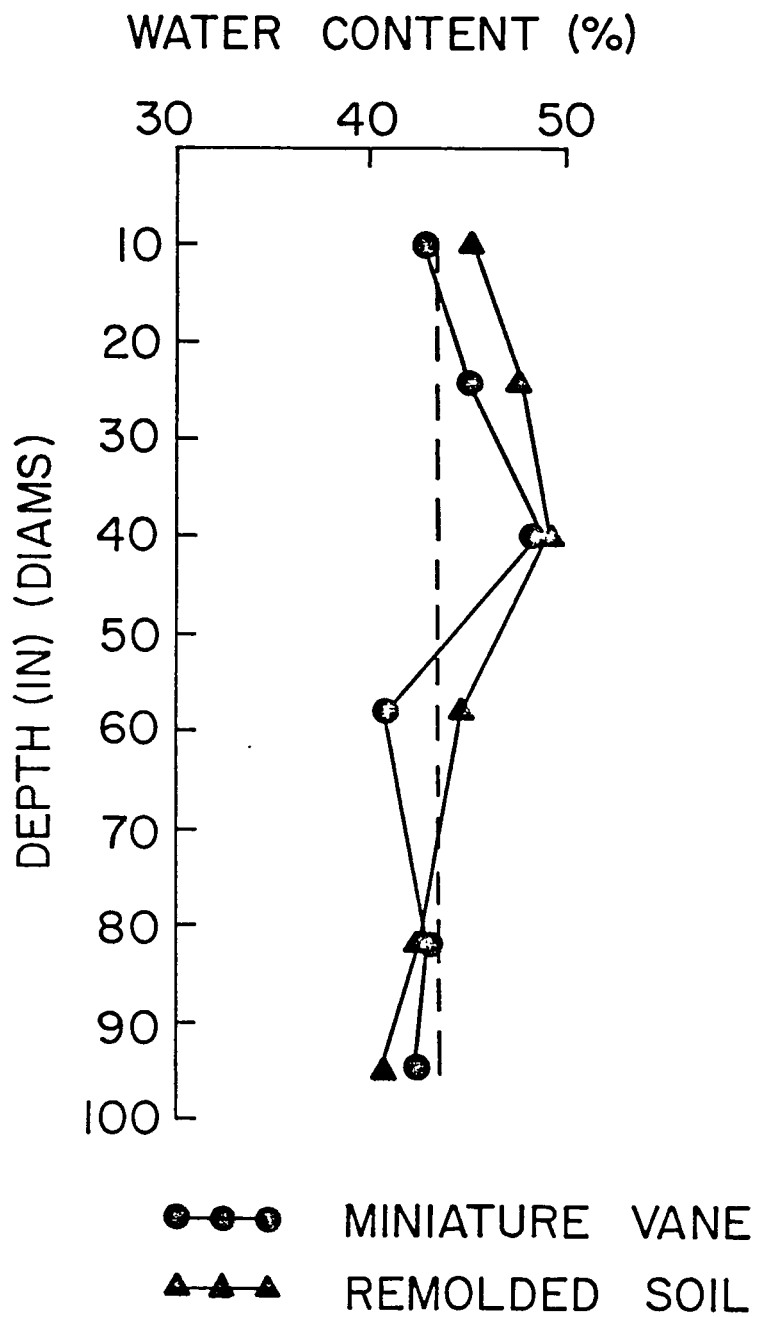


FIGURE 7

Water Content Profile  
Soil II

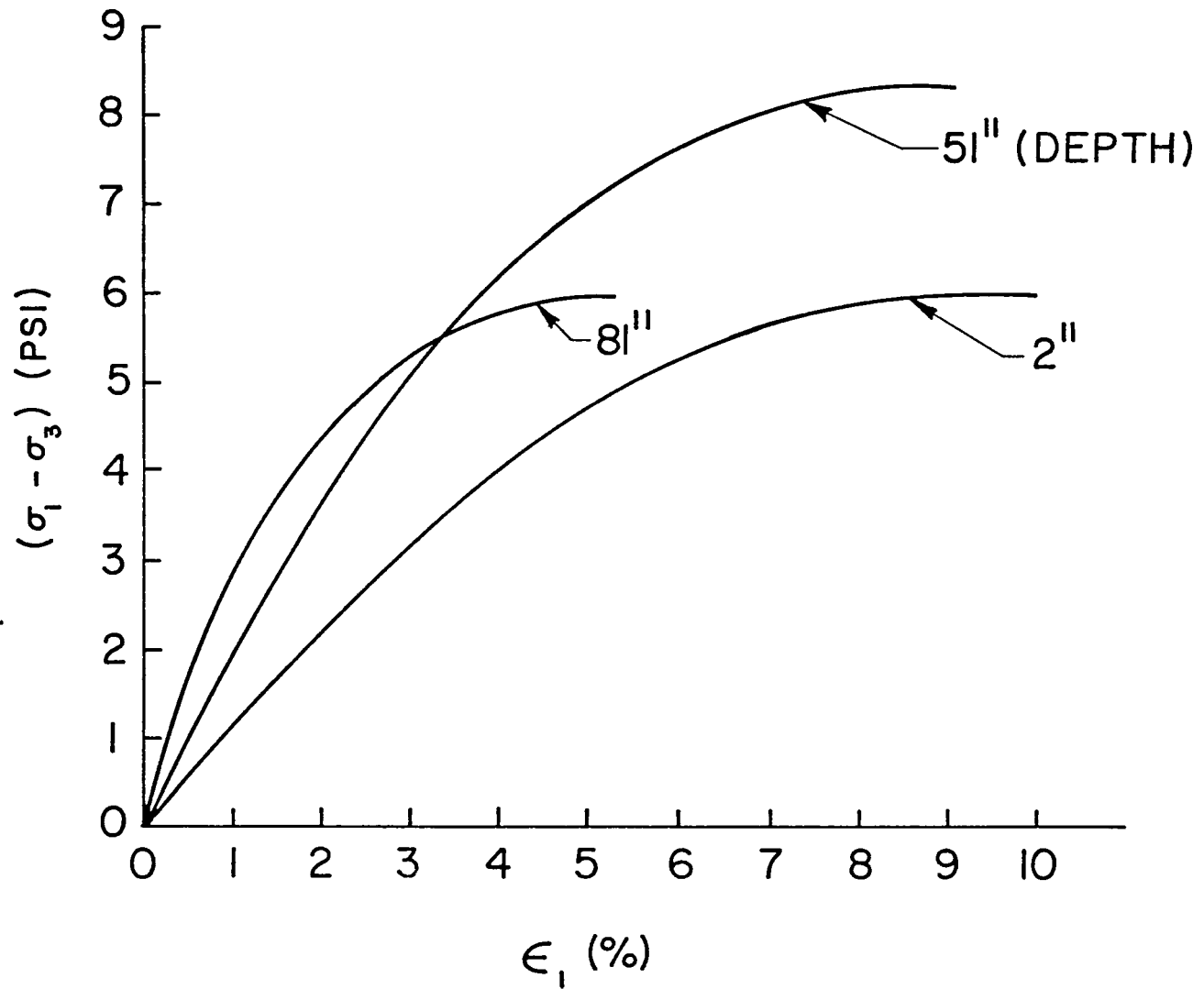


FIGURE 8

Stress-Strain Curves  
Soil I (Remolded)

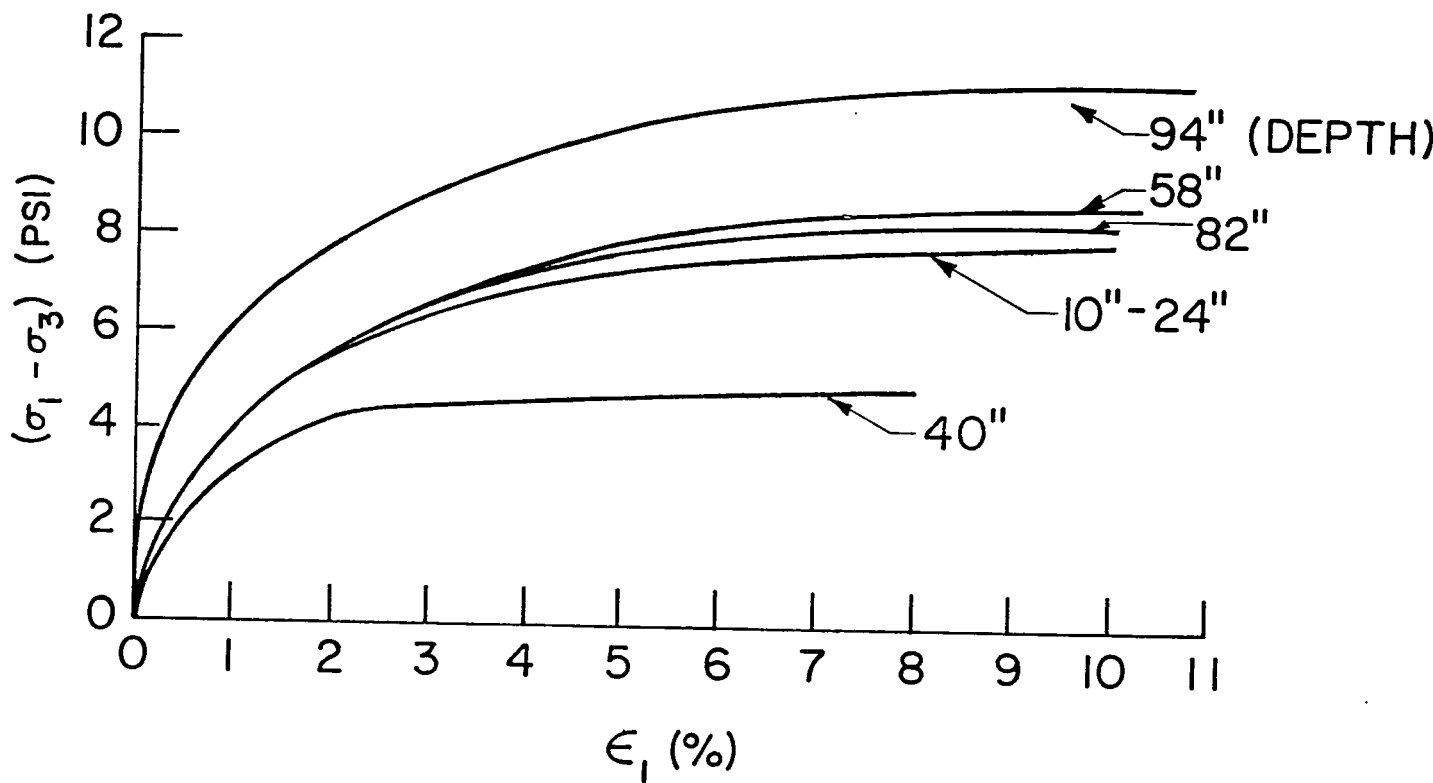


FIGURE 9

Stress-Strain Curves  
Soil II (Remolded)

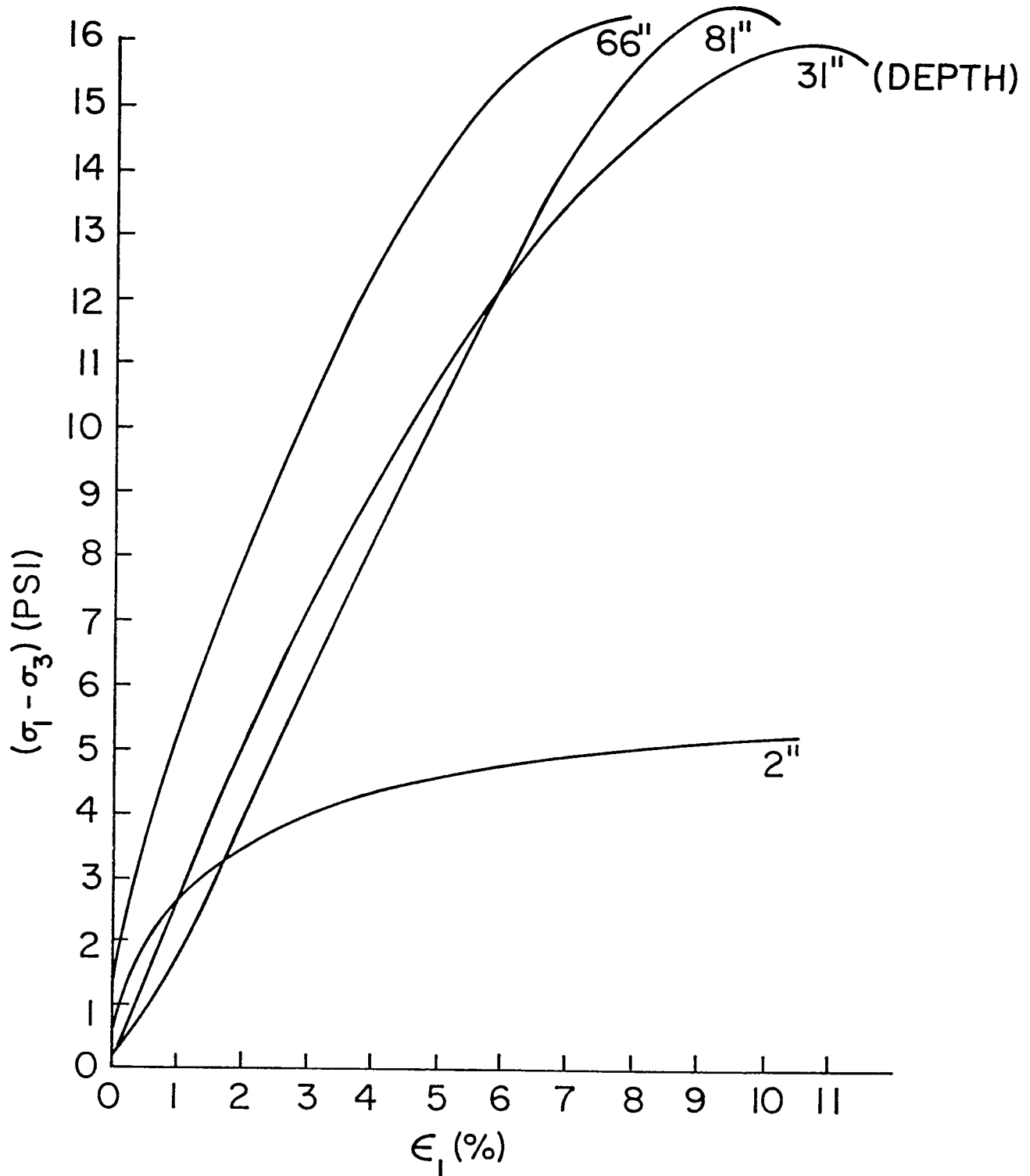


FIGURE 10

Stress-Strain Curves  
Soil I (Undisturbed)

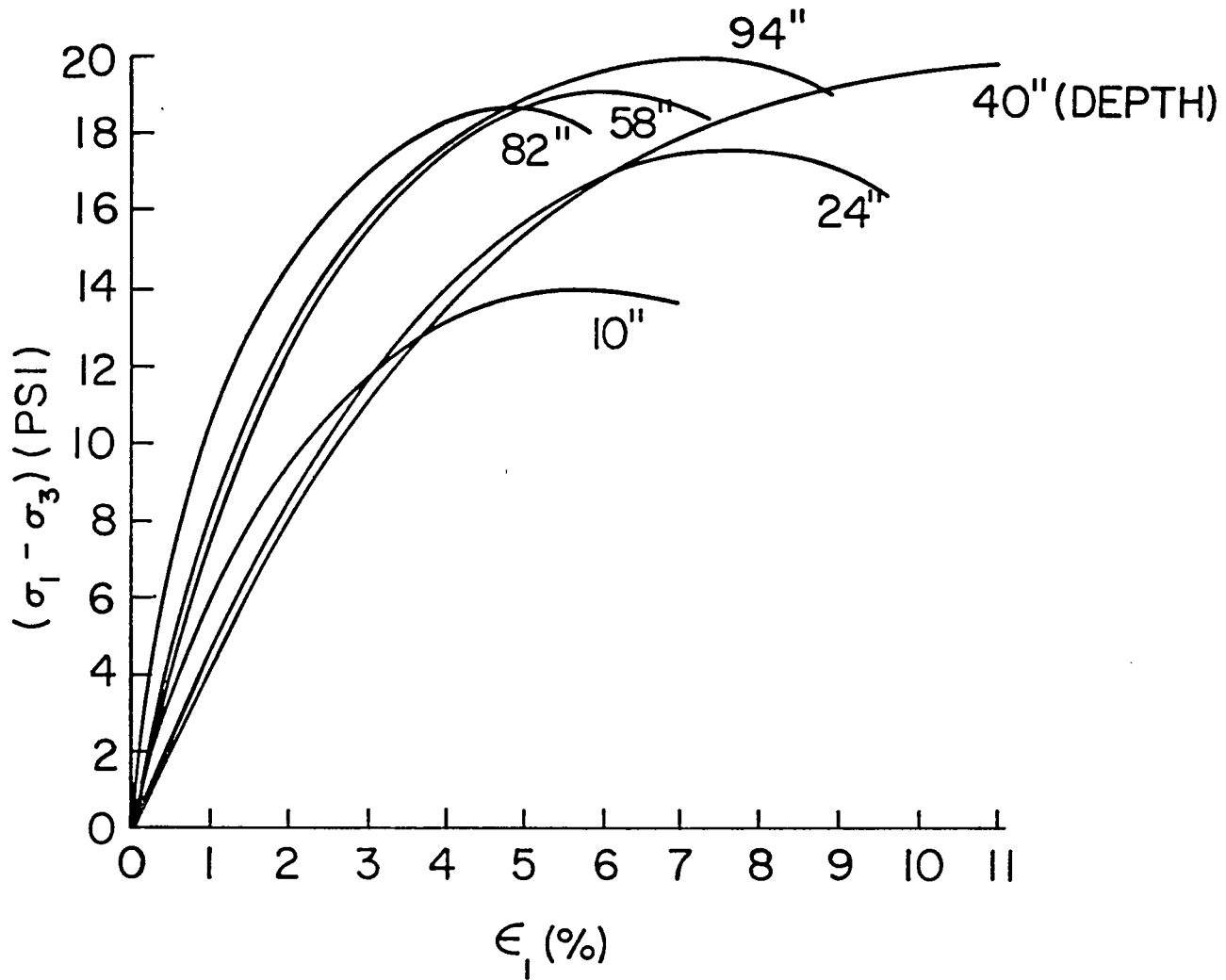


FIGURE 11

Stress-Strain Curves  
Soil II (Undisturbed)

CHAPTER III  
TESTING PROGRAM

Instrumentation

The instrumentation for this study consisted of five (5) instrumented pile sections, a switch and balance box, strain indicator, amplifiers, and a four-trace oscilloscope. The five pile sections were made from 1-inch O.D. machine tubing having a .096-inch wall thickness. Each section was 21 inches long, giving a total pile length of 105 inches. The sections were numbered one through five, with section one being the bottom section. Both ends of the pile sections were threaded internally and joined together with nipples. This allowed load tests at four different L/D ratios and four consequent values of relative stiffness. Each pile segment was instrumented with two strain gauges, which were placed internally at the top of each pile segment. The bottom pile section was instrumented with two additional gauges placed symmetrically at the bottom end of the section. This gave a total of six gauge locations for the complete piles. Lead wires from the gauges were brought out through the center of the pile. A full bridge was completed externally by placing the active gauges in opposite arms of the bridge and wiring precision resistors, contained in a buried pipe, into the remaining arms of the bridge. By keeping the compensating

arms of the bridge in the ground near the pile, the lengths of the lead wires for all four arms of the bridge were equalized and the temperature compensation of the system was improved. The completed bridges were then wired into the switch and balance box. The output from the bridges was read sequentially during a load test, using a strain indicator. The compression in the pile during driving was monitored using the oscilloscope. Fig. 12 shows a schematic of the instrumentation and wiring. Typical traces obtained from the oscilloscope during driving are shown in Fig. 13.

One-hundred-twenty ohm gauges were used for both tests. For the first test, W. T. Bean strain gauges (type BAE-06-250BB-120TE) were used. Eastman 910 was used as the adhesive, and Gage Coat 3 and Gage Coat 5 were used as waterproofing. For the second pile, Micro-Measurements strain gauges (type EA-06-250BG-120) were used. M-Bond AE 15 was used as both the adhesive and waterproofing.

Each pile segment was calibrated in a testing machine in order to obtain a direct relationship between gauge output and load for later use in reducing the data. Calibration also provided an opportunity to examine drift in the instrumentation system and to take steps to reduce drift to a minimum.

#### Testing Frame and Soil Column

The soil for the test was compacted with a pneumatic backfill tamper inside three fifty-five gallon drums. When

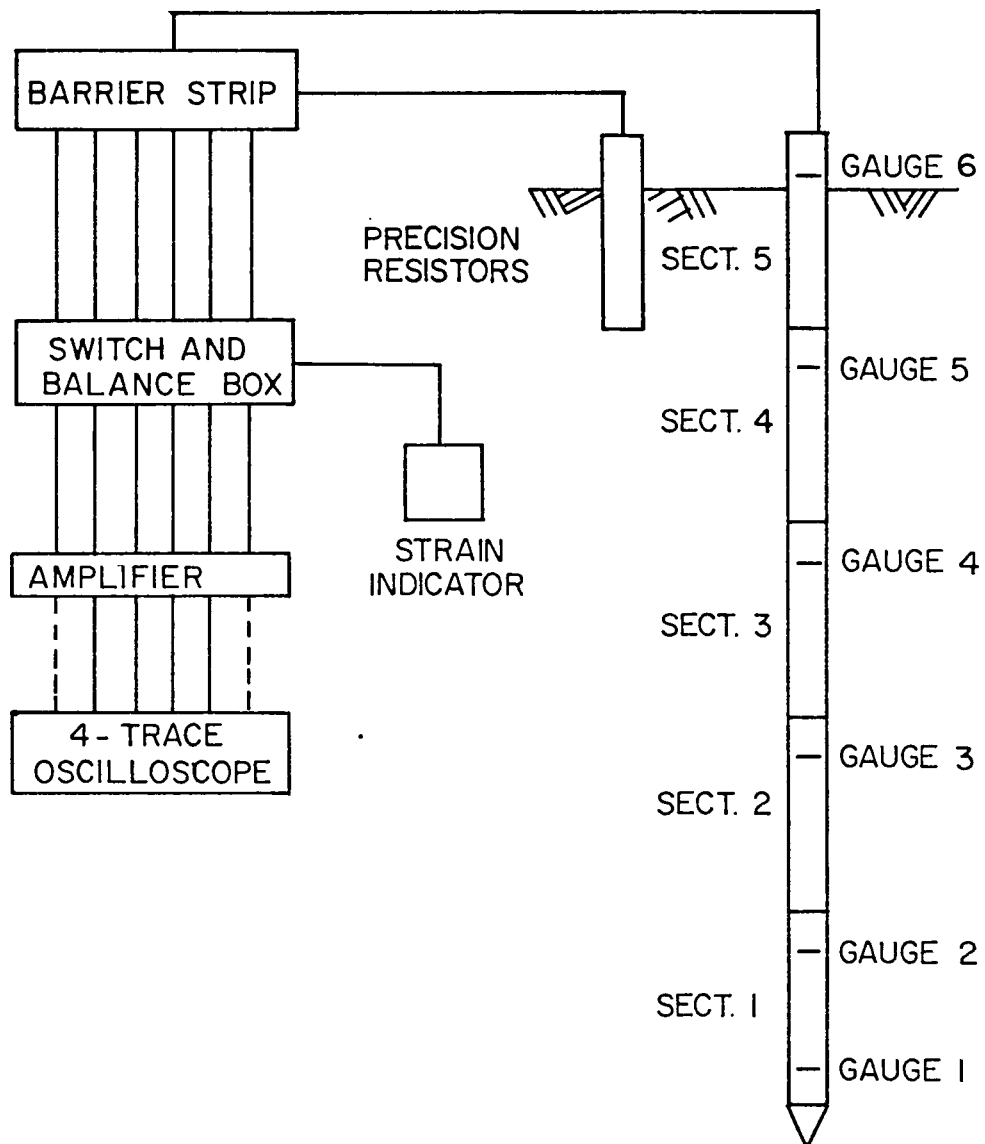
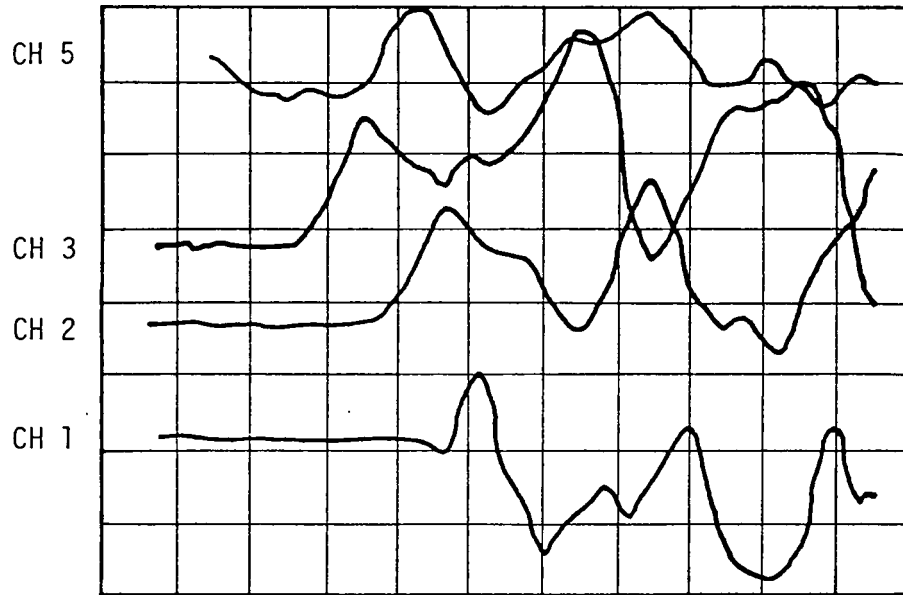
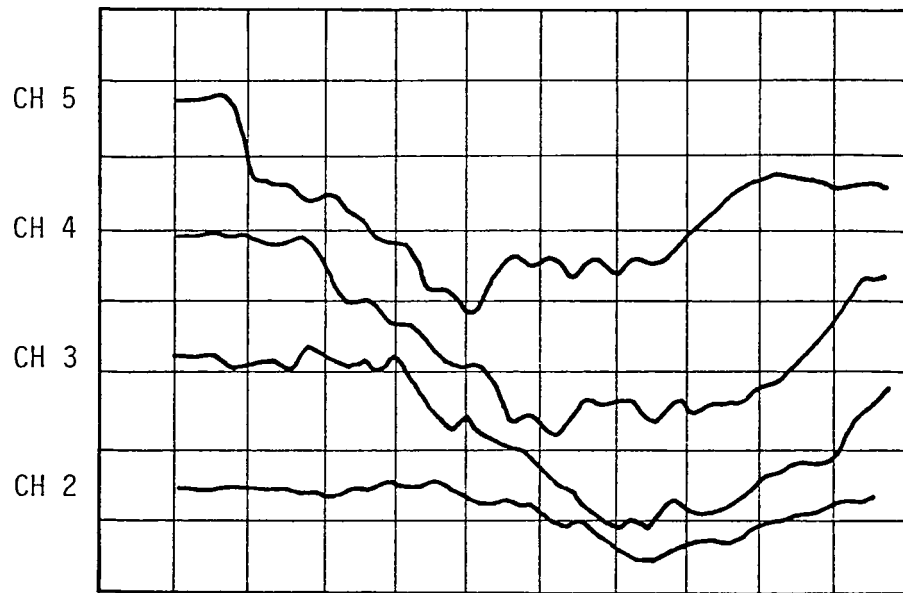


FIGURE 12

Schematic of Instrumentation



Soil II - 82" Penetration  
25 ft-lb - 9 Blows/In.



Soil I - 84" Penetration  
25 ft-lb - 15 Blows/In.

Figure 13

the first drum was full, a second drum was placed on top of it and held in place with a steel ring. A heavy grease was used to make the joint watertight. The third drum was spot welded into place when the second drum was full. A heavy grease and duct tape were used to make the seal watertight. The total height of the three drums was 105 inches. The soil was compacted to a depth of approximately 100 inches.

A reaction frame was constructed to fit around the drums. The purpose of the frame was to position the driving hammer and provide a reaction beam for the load tests. Figure 14 gives an overall perspective of the test arrangement.

#### Driving System

The driving system consisted of four pieces: a transition piece, a driving plate, a guide tube, and a drop hammer. The cylindrical drop hammer was machined from a solid steel bar to weigh 25 pounds and to fit precisely into the guide tube, which was machine tubing with a slightly larger inside diameter than the outside diameter of the hammer. The pile was driven by dropping the hammer known distances inside the guide tube onto a steel driving plate attached to the pile head. The guide tube fit into a groove machined into the driving plate, which kept the hammer centered over the pile while the pile was being driven. The guide tube was kept vertical by lateral bracing within the crown section of the

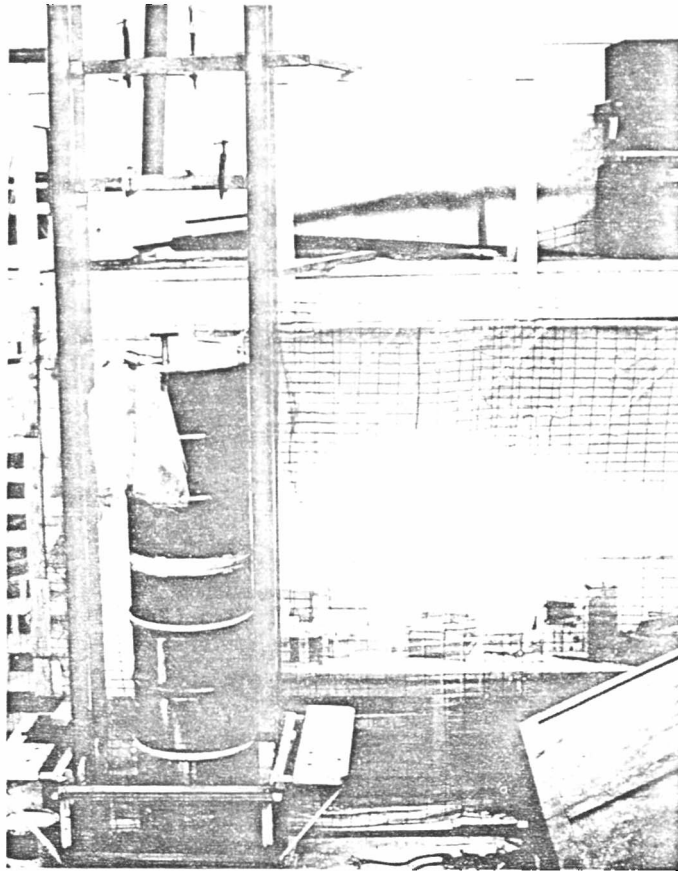


FIGURE 14  
OVERALL TEST SET-UP

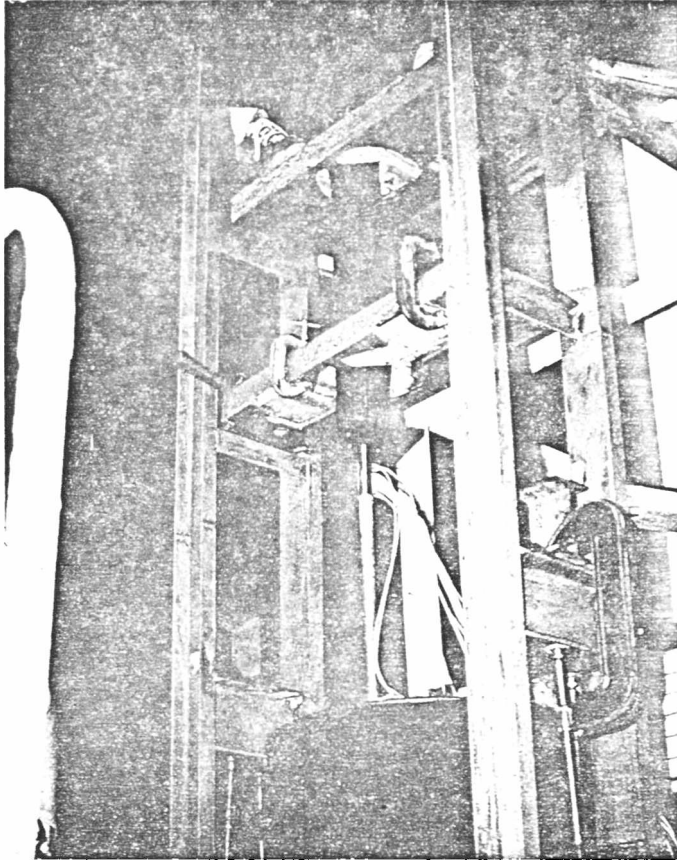


FIGURE 15  
THE DRIVING SYSTEM



FIGURE 16

THE LOADING AND SETTLEMENT  
MEASUREMENT DEVICES

reaction frame. A transition piece was placed between the driving plate and the top of the pile. Its purpose was to provide a space for the strain gauge wires to pass out of the pile. The driving system is depicted in Fig. 15.

### Loading System

The pile was loaded by using a small ram activated by a hydraulic jack. The ram was centered over the pile on the driving plate, which remained in position after driving to serve as a loading head for the ram. An instrumented proving ring was placed on top of the ram to measure the applied load. A loading ball was placed between the proving ring and the reaction beam. The ram, proving ring, and loading ball were all centered over the pile by eye to limit any eccentric loads. The reaction beam was temporarily attached to the reaction frame with C-clamps and was removed when new segments of piling were being driven. A photograph of the loading system is presented in Fig. 16. The strain gauge location of the top pile section was always maintained just above the soil surface so the load applied to the pile could be measured at that location as well as at the proving ring, as a means of verifying the proving ring reading.

The entire test apparatus was situated inside a shop building on the University of Houston campus, in order to minimize effects of environmental changes on the performance of the instrumentation.

## Testing Procedures

The test pile was installed in five sections, and axial load tests were conducted in each soil at four successively greater penetrations. The first pile section was placed in an undersized, pre-drilled hole in order to insure that the pile initially penetrated as vertically as possible. No load tests were run at that depth. The first load test was run after the second segment had been attached and driven to an L/D ratio of 36. The remaining tests were run at L/D ratios of 58, 78, and 97. A reservoir of free water was placed on the surface through which the pile was driven in order to simulate offshore driving conditions. This allowed water to penetrate the gap at the pile-soil interface generated during driving. Load tests were conducted immediately after driving and again after 24 hours. The testing was conducted in the following sequence: A new pile section was added to the pile already in the ground. The strain gauge bridges were hooked up and checked. The driving system was placed on the pile. The pile was driven with 25 ft-lbs of energy per blow. The penetration rate varied from about 5 blows per inch at a penetration of 40 inches to a maximum of 15 blows per inch at a penetration of 97 inches in both soils. A plot of the measured blow count vs. penetration for both soils is shown in Fig. 17. When the pile had been driven to the desired depth, the driving system was removed and the loading system was

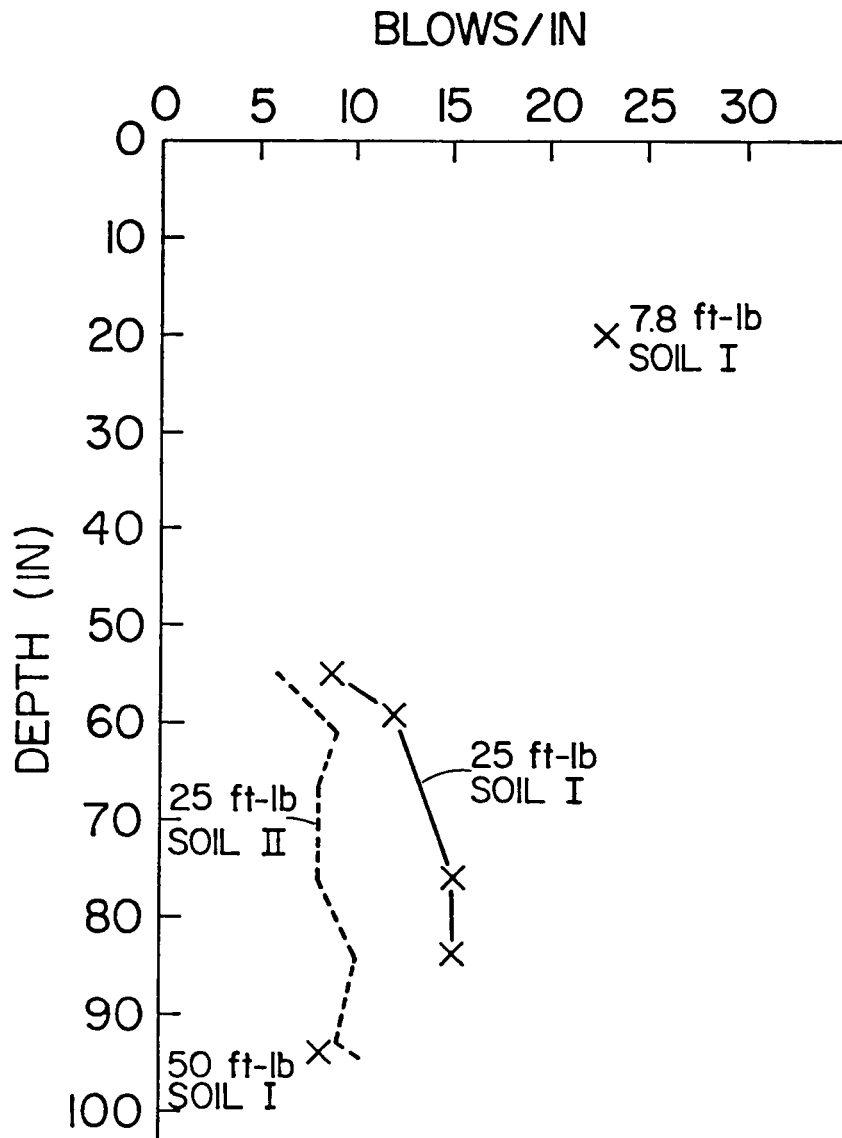


Figure 17  
Blow Count vs Depth

installed. The process consisted of positioning the reaction beam and placing and aligning the ram, proving ring, and loading ball. This process usually took about 30 minutes. The pile was then loaded to failure without delay. The loading procedure followed was similar to the quick test method prescribed by the Texas Highway Department (Ref. 10). Successive loads were applied in small increments and held for 2.5 minutes until the pile failed by plunging. The pile was failed in approximately 30 minutes in each test. The gauge outputs were recorded at all gauge locations, and the settlement at the top of the pile was measured with two dial gauges. Figure 16 shows the arrangement of the loading and settlement measuring devices. Strain gauge readings were taken as quickly as possible during every load increment in order to provide an instantaneous picture of load distribution in the pile, which is essential as the pile approaches failure. Another test was run 24 hours after driving to determine if any changes due to set-up could be detected.

During the driving of the piles, the output from the strain gauges was monitored on a four-trace oscilloscope. The scope was set to trigger when the stress pulse from the drop of the hammer reached the first gauge location. As the stress wave reached each succeeding gauge location, the output from the strain gauge bridge was displayed on the oscilloscope

and recorded with a Polaroid camera. An example of the data taken is shown in Fig. 13. In order to interpret the data, it was necessary to assume that for a given compressive stress, the outputs of the strain gauge bridges were equal. This assumption was verified by the pre- and post-test calibration constants determined for static conditions.

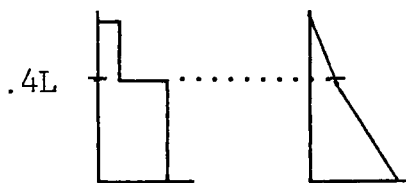
## CHAPTER IV

## PRESENTATION OF RESULTS

For this analysis, the hammer-pile-soil system was modeled at penetrations of 20, 60, 80, and 95 inches. Several computer runs were made at the 95-inch penetration in order to determine what set of parameters best modeled the test piles. Once these parameters were evaluated, the model was analyzed at 80, 60, and 20 inches of penetration to see if any length dependency could be shown. The results of these computer runs are presented in tables I through V. For each pile penetration, a standard case was also run. For the standard case, the damping constants were taken as the values recommended in the wave equation program manual (Ref. 6). The side damping was taken as 0.2 sec/ft, and the tip damping was 0.01 sec/ft. The distribution of the side damping was assumed to be uniform along the embedded length of the pile; that is, each discrete element was assigned a J value of 0.2. The static soil resistance was also distributed uniformly along the pile with ten percent of the total resistance applied at the tip. The value of  $R_u$  (total), the total soil resistance, was measured by static load tests conducted at each penetration for which the wave equation analysis was made (except 20 inches) immediately after driving to that penetration. During the

TABLE I  
SOIL I - 97-INCH PENETRATION

J (aver.)	Distribution		Depth	Stress Ratio		Blows/in	
	Damping	Soil Resis.		Calc.	Meas.	Calc.	Meas.
.2	Uniform	Uniform	39"	100	100	2.7	8
			57"	94	95		
			77"	79	47		
				(91%)	(81%)		
.5	Uniform	Uniform	39"	100	100	4.7	8
			57"	91	95		
			77"	73	47		
				(88%)	(81%)		
1.0	Uniform	Uniform	39"	100	100	7.8	8
			57"	86	95		
			77"	63	47		
				(83%)	(81%)		
1.0	Propor.*	Propor.*	39"	100	100	8.8	8
			57"	77	95		
			77"	50	47		
				(75%)	(81%)		



\*Damping vs. Depth      \*Soil Resis. vs. Depth

Note: Values in parentheses are average values of the stress ratio.

TABLE II  
SOIL II - 97-INCH PENETRATION

J (aver.)	Distribution		Depth	Stress Ratio		Blows/in	
	Damping	Soil Resis.		Calc.	Meas.	Calc.	Meas.
.2	Uniform	Uniform	19"	100	100	3.9	10
			39"	93	90		
			57"	88	82		
			77"	74	63		
				(89%)	(84%)		
.75	Uniform	Uniform	19"	100	100	8.5	10
			39"	88	90		
			57"	79	82		
			77"	62	63		
				(82%)	(84%)		
.75	Propor.	Propor.	19"	100	100	10.0	10
			39"	98	90		
			57"	91	82		
			77"	62	63		
				(88%)	(84%)		

Note: Values in parentheses are average values of the stress ratio.

TABLE III  
SOIL I - 80-INCH PENETRATION

J (aver.)	Distribution		Depth	Stress Ratio		Blows/in	
	Damping	Soil Resis.		Calc.	Meas.	Calc.	Meas.
1.0	Uniform	Uniform	10"	100	100	12.3	15
			31"	84	90		
			52"	63	68		
				(82%)	(86%)		
1.0	Propor.	Propor.	10"		100	13.3	15
			31"		90		
			52"		68		
					(86%)		

Note: Values in parentheses are average values of the stress ratio.

TABLE IV  
SOIL II - 80-INCH PENETRATION

J (aver.)	Distribution		Blows/in	
	Damping	Soil Resis.	Calc.	Meas.
.2	Uniform	Uniform	3.8	9
.75	Uniform	Uniform	8.2	9
.75	Propor.	Propor.	9.5	9

TABLE V  
SOIL II - 60-INCH PENETRATION

J (aver.)	Distribution		Blows/in	
	Damping	Soil Resis.	Calc.	Meas.
.2	Uniform	Uniform	3.5	8.5
.75	Uniform	Uniform	7.4	8.5
.75	Propor.	Propor.	8.8	8.5

computer analysis, three variables were examined to determine which combination provided the best correlation with the measured data. These variables were first, the magnitude of the average damping constant, second, the distribution of the damping along the pile, and third, the distribution of the soil resistance along the pile. The procedure used to determine the best combination of these variables was as follows. First, the average damping parameter was varied with the distribution of side damping and soil resistance kept uniform. Once a value of damping was found that tended to make the computed blow counts and stress propagation pattern approach the measured values for given soil and penetration conditions, the distributions of side damping and soil resistance were altered to duplicate the pattern of load transfer obtained from the static tests. In altering the distribution of the damping, the same average value of the damping constant was maintained. By altering the distributions of damping and soil resistance, the computed blow counts were increased by an average of 12% for all penetrations examined. The best computer model was obtained with the damping and soil resistance distributed according to the load-transfer curves.

The stress ratios and blow counts presented in tables I through V were used as the criteria for determining if the computer had properly modeled the test piles. The

term "stress ratio" is defined as the ratio of peak stress at a given gauge location to that at a reference location, usually the first level below the soil surface. Stress ratios represent the decay of the first compressive stress wave as it passes down the pile.

The measured stress ratio was obtained from the polaroid pictures taken during the driving of the pile. The maximum output from the reference gauge location was taken as 100%, and the relative magnitude of the stress wave at the lower levels in the pile was determined as a percentage of that value. Due to the complex wave geometry caused by the reflected waves, no meaningful data could be obtained for the passage of subsequent waves. The calculated stress ratio was computed from the computer output by using the maximum compressive stress in each element that occurred during the first pass of the stress wave. The measured and computed stress ratios were compared at equivalent locations on the pile to determine how well the computer solution modeled the damping of the stresses as the wave passed down the pile. The wave equation model indicated that approximately 12 passes of the compression wave occurred before the pile tip stopped penetrating.

The output from the computer program indicated that the maximum compressive stress in each segment of the pile occurred during the first pass of the compressive wave. The

only exception was when very high damping parameters were used near the bottom of the pile. Use of these high damping parameters at the tip ( $J_{av} = 2.5$ ) resulted in the maximum compressive stress occurring during the second pass of the stress wave. Since the computed blow counts were too high, this was obviously not a good model of the test pile. With such high damping at the tip, the wave equation model would seem to be simulating an end bearing rather than a friction pile.

As can be seen from the tabulated results, the agreement on blow count could be made quite good; however, the stress ratio could only be brought into approximate agreement. It is logical that the average stress ratio is related to the amount of energy in the pile after the passage of the first stress wave and that, if the calculated and measured average stress ratios are the same, the respective blow counts should be equal. However, since the data are for only the first pass of the stress wave, and the computer solution indicates that the stress wave will pass up and down the pile several times, exact agreement is not to be expected. Additionally, these discrepancies are due not only to the data but also to the assumptions made in setting up the computer algorithm for damping. Specifically, the damping constant  $J(m)$ , which is explicitly a viscous damping term in the algorithm, is used to represent both viscous and frictional damping in the real soil. In light

of these limitations, the agreement in stress ratios achieved seemed the best attainable without altering the algorithm and rerunning the tests, both of which are outside the scope of this project.

As can be seen from tables III through V, the agreement with the test results on the 80-inch and 60-inch penetrations was reasonably good. Using the average damping values obtained at the 95-inch penetration and distributing the damping and soil resistance in proportion to the measured soil resistance, the average predicted blows/inch were within 7% of the measured values. At the 20-inch penetration, however, the agreement with the measured values was very poor, although static capacity was not determined at the 20-inch penetration. The established damping constant and proportional distribution were used to obtain a computer solution to determine the equivalent static capacity that corresponded to the measured blow-count and hammer energy. The wave-equation-predicted capacity was near 450 lb. This value was unreasonable since the measured capacity at almost three times the penetration was only 390 lb. To bring the computed blow counts up to the measured values at a reasonable value of static capacity would have required a damping parameter significantly greater than 1.0, the value used in the analysis. It was concluded then that the computer model using this value of damping parameter breaks down at the shallow penetration.

## CHAPTER V

### DISCUSSION AND RECOMMENDATIONS

To date, several authors have published data indicating appropriate values for the wave equation damping parameter. Smith (Ref. 11), in his original paper on pile driving analysis using the wave equation, recommended values of side damping and point damping of 0.05 and 0.15 sec/ft, respectively. He stated that these values were based on his experience, and more appropriate values should be used when they became available. Since that original paper, several Texas Transportation Institute research reports have attempted to refine these values. Lowery et al. (1969, Ref. 7) indicated in their state-of-the-art report that the point damping parameter in clay should be 0.3, and the side damping parameter should be 0.1. These values were reported to vary by  $\pm 50\%$ . In a later report by Van Reenen et al. (1971, Ref. 12), the side damping parameter for piles driven in Beaumont Clays was reported to be 0.2 and the tip damping was zero. An earlier paper by Forehand and Reese (1964, Ref. 5) indicated that good correlation with field load tests was made using a point damping parameter equal to 1.0 and a side damping parameter equal to 0.33. Corb and Coyle (1969, Ref. 2) reported field test results on small instrumented piles that indicated that the damping parameter varied with the

instantaneous velocity of the pile. They reported that, by raising the velocity to some power  $N$ , the damping parameter remained constant over the velocity range of 0-12 ft/sec. Their reported values for clay were:

$$\begin{array}{ll} J \text{ (side)} = 1.25 & J \text{ (point)} = 0.15 \\ N \text{ (side)} = 0.35 & N \text{ (point)} = 1.00 \end{array}$$

It was also reported by Bartoskewitz and Coyle (1970, Ref. 1) that the damping parameter was not a constant for all soils. They reported an inverse relationship between plasticity index ( $I_p$ ) and damping. This trend was also observed in the present tests. For Soil I, with an  $I_p$  equal to 23, an average side damping parameter of 1.0 gave the best correlation; and for Soil II, with an  $I_p$  equal to 37, an average side damping parameter of 0.75 gave the best correlation. Since the values of damping reported by Bartoskewitz and Coyle were based on the modified representation of damping presented by Corb and Coyle, it was not possible to make any direct comparisons between their reported values of damping parameters and the ones developed in this study.

In addition to the variation of the reported value of the damping parameter, there is also disagreement as to the relative importance of side damping and point damping. Smith (Ref. 11) initially indicated that point damping was of primary importance and that side damping should be taken as

just one third of the point damping. Forehand and Reese (Ref. 5) concur with this, reasoning that the point damping involves "pushing the soil aside at the pile tip, resulting in a 'viscous' action." On the other hand, Bartoskewitz and Coyle (Ref. 1) state that the parametric studies they conducted indicated the point damping had no significant influence on the accuracy of predicted bearing capacities of friction piles in clay.

It is quite apparent, even from this cursory review of the published information, that the damping parameter is anything but well defined. The reason for this is that the development of resistance along a pile during driving is an extremely complex phenomenon, and it is beyond the present state of the art to quantitatively evaluate all of the significant parameters. The results of this present study are by no means definitive and are not recommended for field application without substantial corroborating evidence. However, it is possible to gain some insight into the problem from the small scale tests run in this program. The values of average damping that gave the best correlations were 1.0 for the low plasticity soil ( $I_p = 23$ ) and 0.75 for the soil with the higher plasticity ( $I_p = 37$ ). In both models, the damping and soil resistance were distributed according to the static load transfer curves. The values of the damping parameters obtained in these tests are higher than

any reported in the literature for clays (with the exception of those reported for the modified representation of viscous damping). A possible explanation for this phenomenon is that the damping parameter is dependent on the frequency of the stress cycle applied to the soil along the pile. The higher the frequency (i.e., the shorter the pile), the higher the damping constant will be. The rather simplistic reasoning behind this proposal is as follows. In the computer model, the viscous damping force is proportional only to particle velocity of the pile segment. The computer solution does not take into account the frequency of the loading of the soil as the stress wave passes a pile section. It is well established from elastic theory that soil damping is frequency dependent. For example, Novak (Ref. 8), in his paper, "The Dynamic Stiffness and Damping of Piles," clearly shows this dependency. He presents an equation for the vertical damping of a single pile and shows that it is dependent on both  $a_0$  (the dimensionless frequency ratio) and  $\Lambda_2$  (a complex frequency parameter). It would seem reasonable, then, that the damping parameter in the computer solution should be frequency dependent also. That is to say, the solution given from the present version of the wave equation analysis would be strictly correct for only one frequency of soil loading. Therefore, the damping parameter would be expected to vary from one case to another as the frequency of soil loading

changed. For a given pile material and soil stratigraphy, the parameter that controls the frequency of soil stress loading is the pile length. For short piles, that frequency would be relatively high, as stress waves reflect rapidly up and down the pile. The computer analysis conducted showed that the stress wave passed each point on the pile approximately 12 times in the 0.001 seconds of real time simulated in the solution (i.e., high frequency loading). Soil damping at high frequencies is high; and, as might be expected, high damping parameters were found to provide the best correlations. When the same damping parameters were applied to the pile at the 20-inch penetration, it was evident that these damping parameters were too low to produce good correlations. At the other end of the spectrum, the damping for extremely long piles should be less than the typical values which were developed from piles that were generally less than 100 feet long. Although no data regarding this point are known to have been published, it is interesting to consider the experience of Exxon Company during the installation of the pile foundations for the Hondo platform. The pile foundations of this structure contained the longest single pile ever driven. It was 1255 ft long and was driven to 375 ft penetration into a stiff-to-hard gray silty clay. In the paper presented by Cunningham and Naughton (Ref. 4), the authors indicate an initial concern over the ability to drive

the long piles required. The primary hammer selected was the Vulcan 3100, which has a rated striking energy of 300,000 ft-lbs. A larger backup hammer was also on site, the Menck MRBS 4600, which has a rated striking energy of 500,000 ft-lbs. Driving was observed to be easier than anticipated, and the larger Menck hammer was not required. According to the hypothesis set forth in this chapter, the extreme length of the pile resulted in a relatively low frequency loading of the soil along the pile by the stress wave. The soil produces a much lower damping of the energy in the pile at this frequency and, therefore, the pile would be expected to drive more easily than predicted using the standard damping parameters.

It should be reiterated that this hypothesis is based on only a small amount of data. It is recommended that future work be done to investigate its validity and significance, if any, and to quantify the actual relationship between damping and frequency. Specific areas of work could be in the development of the theoretical model of the vibrating pile-soil system. Perhaps an avenue that would provide more immediate results would be a correlation of wave equation analyses and driving records with pile lengths from published data. However, if this course is taken, it would be well to note the experience of Tavenas and Audibert (Ref. 9). They achieved very good correlations of driving records and wave

equation analysis on their test piles driven under tightly controlled circumstances. However, the correlations with production piles driven in the same formation were not good. The reason given was the variation of other parameters during driving that could not be predicted in the computer analysis. Therefore, if field data are to be correlated, only data with all the variables accurately reported should be considered, so as not to mask the phenomenon of a variable damping coefficient.

## BIBLIOGRAPHY

1. Bartoskewitz, R. E., and Coyle, H. M., "Wave Equation Prediction of the Pile Bearing Capacity Compared with Field Test Results," Texas Transportation Institute Research Report 125-5, December, 1970.
2. Corb, K. W., and Coyle, H. M., "Dynamic and Static Field Tests on Small Instrumented Piles," Texas Transportation Institute Research Report 125-2, February, 1969.
3. Coyle, H. M., Foye, R., and Bartoskewitz, R. E., "Wave Equation Analysis of Instrumented Test Piles," Proceedings, 5th Annual Offshore Technology Conference, Vol. II, May, 1973.
4. Cunningham, G. R., and Naughton, H. R., "Design and Installation of the Piling Foundation for the Hondo Platform in 850 Feet of Water in the Santa Barbara Channel," Proceedings, 1977 Offshore Technology Conference, Vol. II, May, 1977.
5. Forehand, P. W., and Reese, J. L., "Predictions of Pile Capacity by the Wave Equation," Journal of the Soil Mechanics and Foundation Division, A.S.C.E., Vol. 90, No. SM2, 1964.
6. Hirsch, T. J., Carr, L., and Lowery, L. L., "Pile Driving Analysis - Wave Equation Users Manual TTI Program," Federal Highway Administration Report FHWA-IP-76-13.3, April, 1976.
7. Lowery, L. L., Husch, T. J., Edwards, T. C., Coyle, H. M., and Samson, C. H., "Pile Driving Analysis State of the Art," Texas Transportation Institute Research Report 33-13, Texas A & M University, 1969.
8. Novak, M., "Dynamic Damping and Stiffness of Piles," Canadian Geotechnical Journal, Vol. 11, 1974.
9. Tavenas, F. A., and Audibert, J. M. E., "Application of the Wave Equation Analysis to Friction Piles in Sand," Canadian Geotechnical Journal, Vol. 14, February, 1977.

10. \_\_\_\_\_, "Foundation Test Loads," Texas Highway Department Standard Specifications for Construction of Highways, Streets and Bridges, Item 405, January, 1972.
11. Smith, A. E. L., "Pile Driving Analysis by the Wave Equation," Journal of the Soil Mechanics and Foundations Division, A.S.C.E., Vol. 86, No. SM4, August, 1960.
12. VanReenen, D. A., Coyle, H. M., and Bartoskewitz, R. E., "Investigation of Soil Damping on Full Scale Test Piles," Texas Transportation Institute Research Report 125-6, Texas A & M University, August, 1971.

APPENDIX I  
SOIL CHEMICAL ANALYSIS

Kaolin - P

<u>Compound</u>	<u>% Weight</u>	
Al <sub>2</sub> O <sub>3</sub>	25.30	Free Moisture .7-.9% wt.
SiO <sub>2</sub>	49.00	Specific Gravity 2.58
Fe <sub>2</sub> O <sub>3</sub>	0.75	0% Retained on 200 mesh
TiO <sub>2</sub>	0.65	2% Retained on 325 mesh
CaO + MgO	0.50	
NaO + K <sub>2</sub> O	1.00	
L.O.I.	12.50	

Bascogel

<u>Compound</u>	<u>% Weight</u>	
SiO <sub>2</sub>	55.1	Free Moisture 11%
Al <sub>2</sub> O <sub>3</sub>	23.3	0% Retained on 200 mesh
MgO	2.9	2% Retained on 325 mesh
CaO	4.7	
NaO	1.9	
Fe <sub>2</sub> O <sub>3</sub>	1.6	